Title

Photosensitized co-generation of nitric oxide and singlet oxygen Enhanced toxicity against ovarian cancer cells.

Journal

Journal of Nanoparticle Research, 24(4)

ISSN

1388-0764

Authors

Sanchez-Cruz, Pedro

Vazquez, Katerina

Lozada, Eunice

et al.

Publication Date

2022-04-01

DOI

10.1007/s11051-022-05463-x

Peer reviewed

HHS Public Access

Author manuscript

J Nanopart Res. Author manuscript; available in PMC 2023 April 07.

Published in final edited form as:

J Nanopart Res. 2022 April ; 24(4): . doi:10.1007/s11051-022-05463-x.

Photosensitized co-generation of nitric oxide and singlet oxygen Enhanced toxicity against ovarian cancer cells

Pedro Sanchez-Cruz[1], **Katerina Vazquez**[2], **Eunice L. Lozada**[3], **Fatima Valiyeva**[3], **Rohit Sharma**[3], **Pablo E. Vivas**[2,3], **Antonio E. Alegria**[1,*]

[1]Department of Chemistry, University of Puerto Rico, Humacao, PR 00791

[2]Department of Biochemistry, UPR Medical Sciences Campus, San Juan, PR 00936

[3]Comprehensive Cancer Center, UPR Medical Sciences Campus, San Juan, PR 00936

Abstract

Near micromolar concentrations of nitric oxide (NO) induce tumor cells death. However, an appropriate NO load has to be delivered selectively to the tumor site in order to avoid NO loss and secondary NO-induced effects. The encapsulation of millimolar concentrations of a NO source and an appropriate trigger of NO release within phospatidylcholine-based liposomes should provide an efficient tool for the selective release of the needed NO payload. In this work we report the photosensitized generation of singlet oxygen and NO from folate-targeted PEGylated liposomes, containing AlPcS4 as the sensitizer and *S*-nitrosoglutathione (GSNO), in millimolar amounts, as the NO source. Amounts of singlet oxygen detected outside the liposome when using PEGylated liposomes are near 200 % larger when GSNO is present inside the liposomes as compared to its absence. These liposomes, conjugated to folate, were found to enhance the photosensitized cytotoxicity to A2780CP20 ovarian cancer cells as compared to liposomes containing the sensitizer but no GSNO (30 % as compared to 70 % cell viability) under the conditions of this work. Fluorescense of AlPcS4 was observed inside cells incubated with folate-conjugated liposomes but not with liposomes without folate. The photosensitized activity enhancement by GSNO increased when light fluence or liposome concentration were increased. The majority of ovarian cancer patients are initially diagnosed with disseminated intra-abdominal disease (stages III–IV) and have a 5-year survival of less than 20%. This work suggests a novel ovarian cancer nodules treatment via the use of tumor-targeted liposome nanoparticles with the capability of generating simultaneously reactive oxygen and nitrogen species upon illumination with near-infrared light.

Introduction

Photodynamic therapy (PDT) is one of the noninvasive ways of treating malignant tumors [1] or macular degeneration [2]. It uses a combination of red laser light, a photosensitizing

*Corresponding author: antonio.alegria1@upr.edu (Antonio E. Alegria).

Author Contributions: All authors reviewed the results and approved the final version of the manuscript.

Conflicts of Interest: The authors declare no conflict of interest. The funding sources had no role in study design, data collection, analysis and interpretation or in writing and submitting the manuscript.

agent and molecular oxygen to bring about a therapeutic effect [3]. Singlet oxygen ($^1O_2$) production, the so-called Type II pathway, is claimed as the most important mechanism of PDT which kills tumor cells. However, Type I pathways, i. e. those involving photoreduction or photooxidation of substrates, have also been proposed as photocytotoxic events in PDT, especially in hypoxic environments [4]. However, PDT major disadvantage is that dyes will stay in cells for several weeks [5]. Thus, the skin and eyes become very sensitive to light during this time. If exposed to sunlight or other forms of bright light, the skin can quickly become swollen, sunburned, and blistered. However, liposome encapsulation minimizes PS accumulation in the skin [6]. Several studies have demonstrated a higher accumulation of PSs and better PDT efficacy in tumor tissues for PS-containing liposomes compared to free PSs [6].

For the treatment of pathologies in complex anatomical sites, such as in the peritoneal cavity, where restricted illumination is difficult, improved targeting of the photosensitizer is necessary to prevent damage to the surrounding healthy tissue [7]. Tumor targeting is a modality aimed at decreasing toxic side effects of chemotherapy and at the same time improving tumor tissue damage [8]. Enhancement in PDT of tumor cells by FR-targeted liposomes as compared to non-targeted liposomes has been reported [9]. In addition, PDT in combination to tumor targeting involves double tumor selectivity, since light is also only directed to the desired tissue.

The low PS concentration that accumulates at the tumor site could also be a major limitation of this therapy. However, that limitation can be circumvected by the use of nano carriers such as liposomes. Due to the high payload, a single liposome could theoretically deliver a sufficient amount of PS to a cell to cause lethal oxidative stress following PDT. As a result, less liposomal PS can be administered to patients to achieve equal or larger intratumoral PS levels compared to unencapsulated PS. Polyethyleneglycol (PEG) chains in the outer portions of liposomes protect these particles from being recognized by the mononuclear phagocyte system and thus their fast clearance from the blood stream is avoided [7]. Pegylated liposomes improved the PS uptake and cytotoxicity after irradiation compared to nonpegylated ones in vitro [8,10].

Concentrations of nitric oxide (NO) (>400–500 nM) promote tumor cell cytotoxicity and apoptosis [9,11]. Several papers have described that the combination of NO donors with classical cancer therapies (chemotherapy agents such as cisplatin and doxorubicin, and radiotherapy) enhances the therapeutic outcome of treatment and overcome drug resistance [11–13]. NO can enhance PDT efficacy in hypoxic tumors owing to the ability of NO in freely diffusing into deep hypoxic tumor site [14]. Although PDT in combination with NO is found to improve tumor cell death [15–19], the use of tumor-targeted liposomes encapsulating relatively large concentrations of both NO source and PS has not been reported.

We have examined the co-encapsulation of aluminum phthalocyanine tetrasulfonate, AlPcS4, a hydrophilic PS, and *S*-nitrosoglutathione, GSNO, a hydrophilic nitric oxide source, in pegylated and non-pegylated liposomes in terms of their ability to produce both singlet oxygen and NO. The encapsulation of both the sensitizer and the NO source within

a liposome should increase the probabilities of encounters between the PS excited state and the NO source as well as protects the GSNO from reacting with the outer media. The photosensitized generation of NO from GSNO has been previously reported [20]. AlPcS4 was selected since, being a hydrophilic PS, it can be highly concentrated inside the liposome without the risk of dimerization and thus less possibility of excited triplet state quenching [21]. Furthermore, AlPcS4 (Photosens) is being used in clinical trials in Russia for the treatment of skin, breast, and lung malignancies and cancer of the gastrointestinal tract [22,23]. GSNO was selected in this work for its relatively high water solubility, i. e. 70 mM, and thus its potential for the photosensitized production of toxic concentrations of NO upon light activation. GSNO has also been used in clinical trials investigating its therapeutic efficacy in multiple pathologies and mostly related to its roles in cardiovascular diseases [24]. Since relatively large concentrations of both AlPcS4 and GSNO can be encapsulated in liposomes, the possibilities of absorbing a large number of incident photons and generating micromolar concentrations of both NO as well as singlet oxygen outside the liposomes should occur. In a previous work, a folate-targeted photosensitizer was used in the PDT treatment of intraperitoneal cancer nodules [25]. In addition, a folate-targeted liposome with encapsulated methyl aminolevulinate PSs has been developed for the PDT treatment of ovarian cancer nodules [26]. In the latter work a high payload of PS is obtained at the tumor site, as expected, as compared to non-encapsulated sensitizers. A potential advantage of the formulation presented here, as compared to previous works, is the synergistic behavior in singlet oxygen and NO production of the tumor-targeted nanoparticles as described hereby. We evaluated the *in vitro* PDT performance of these FR-targeted liposomes in the cisplatin resistant human ovarian cancer cells, A2780CP20. The majority of ovarian cancer patients are initially diagnosed with disseminated intra-abdominal disease (stages III–IV) and have a 5-year survival of less than 20% [27]. Thus, it is clinically relevant to find ways of detecting and destroying their metastatic intraperitoneal nodules after reductive surgery. This work propose a potential novel ovarian cancer intraperitoneal nodules treatment via the use of tumor-targeted liposome nanoparticles with the capability of simultaneously generating reactive oxygen and nitrogen species upon illumination with near-infrared light.

Materials and methods

Materials

The PS AlPcS4 was purchased from Frontier Scientific. Phospholipids 1,2-dioleoyl-sn-glycero-3-phosphocholine (DOPC), 1,2-distearoyl-sn-glycero-3-phosphoethanolamine-N-[amino(polyethyleneglycol)-2000] (ammoniumsalt) (PEG), 1,2-distearoyl-sn-glycero-3-phosphoethanolamine-N-[folate(polyethylene glycol)-5000] (ammonium salt) (DSPE-PEG(5000)-Folate) were purchased from Avanti Polar Lipids (Alabaster, AL). Metal chelators DETAPAC and neocuproine were purchased from Alfa Aesar (Tewksbury, MA) and used to avoid transition metal-catalyzed decomposition of GSNO. Cholesterol (CHOL), glutathione (GSH) and all other reagents and solvents were purchased from Sigma-Aldrich Corp (St. Louis, MO). All chemicals were of the highest purity commercially available and were used without further purification. Stock solutions of the dye were prepared in deionized Chelex-treated N_2-saturated water and stored at −20 °C under dark conditions. Deionized and Chelex-treated water was used in the preparation of all stock and sample solutions.

Chelex treatment of water was monitored using the ascorbate test, as described by Buettner. Care was always taken to minimize exposure of solutions to light.

GSNO was synthesized and purified as described by Hart [28]. Briefly, an equimolar sodium nitrite solution was added to a stirred acidified ice-cold glutathione aqueous solution. After 40 minutes the red solution was treated with acetone at 5 °C and the resulting pale red precipitate was filtered off and washed with ice-cold water, acetone and ether. The concentration of GSNO was determined by its absorbance at 334 nm, using the extinction coefficient 767 M^{-1} cm^{-1} [29]. Absorbances were measured using a Hewlett Packard, Diode Array, UV-Vis spectrophotometer.

In addition to avoidance of GSNO decomposition by metal chelators, it has been reported that alkaline pH within the range of 8.4 and 8.8 is the best pH condition to stabilize stored GSNO solutions, at which more than 80 % of the GSNO was preserved after 2 days of storage [28]. Thus, stock solutions of GSNO were prepared in glycine buffer at pH 8.7 and used the same day [28].

Liposome preparation

Liposomes were prepared as reported elsewhere, i. e. by extrusion using an Avanti Mini Extruder (Avanti Polar Lipids) followed by Sephadex exclusion of unencapsulated reagents [6,30,31]. Liposome handling was performed under very subdued light. The following liposomes were prepared (numbers imply mol ratios): 60DOPC:40CHOL, 57.5DOPC:37.5CHOL:5.0PEG and 57.44DOPC:37.44CHOL:5.0PEG:0.13DSPE-PEG(5000)-Folate. Lipid mixtures were dissolved in absolute ethanol and deposited on the walls of a round-bottom flask by evaporation of the solvent under a N_2 flux followed by removal of trace solvent under high vacuum. The dry lipid film (typically containing 10 to 15 μmol of DOPC) was hydrated in 1 ml of glycine-buffered aqueous solution (pH 8.7) containing AlPcS4 and/or GSNO. This was followed by 5 to 10 cycles of freezing with liquid N2 and thawing followed by vortexing. The mixture was then extruded 20 times through two stacked polycarbonate membranes with 200 and 100 nm pores. Non-entrapped solutes were excluded from the liposomes by three Sephadex G-50 spin-column filtrations of this solution [32,33], where the Sephadex columns were saturated with glycine buffer before loading the liposome suspensions in order to avoid pH gradients. Liposomes were used the same day these were prepared.

Encapsulation percent

In order to determine the amounts of dye and GSNO in the liposome, Triton X100 was added to the sample to dissolve and clarify the liposome suspension (100 μLs of liposome suspension in 900 μLs of 10 % Triton X100) [34]. Encapsulation percents were then determined from the ratio of amounts of GSNO and dye within the liposome per mol unit of phospholipid (PL) inside the liposome, after Sephadex extraction of unencapsulated molecules, to the amounts of GSNO and dye, respectively, per mol unit of PL before Sephadex extraction. Dye concentrations were determined spectrophotometrically and GSNO concentrations by HPLC analysis using an Agilent 1100 UV analytical HPLC

chromatograph, as reported previously [35], where the mobile phase used was 0.05% trifluoroacetic acid and methanol (94:6) with a flow rate of 0.75 ml/min and an analytical C18 reversed phase column (Partisil ODS-3, 5-mm particle size, Whatman, Hillsboro, OR) was used as stationary phase. Phospholipid concentrations were determined using the Stewart assay, where the standardbsolutions used were those made with the same lipid mixture of the liposome [36].

Liposome physical characterization

Size measurements were performed via dynamic light scattering using a Mobius dynamic light scattering instrument. Liposome dispersions were diluted with PBS to yield a lipid concentration of 0.25 mg/ml. Determination of zeta potential was carried out with the same instrument, with liposomes suspended in double-distilled water at a lipid concentration of 0.25 mg/ml.

Liposome leakage.—The procedure described by Xie et al. was used for this purpose [37]. A 200 uL aliquot of the irradiated (or non-irradiated) liposome suspension was centrifuged at 10,000 rpm for 10 minutes at 4 °C using a Beckman ultracentrifuge (Optima LE-80, Beckman Instruments Inc., Palo Alto, USA) with temperature-control capability. Aliquots of 50 uLs of the supernatant were then analyzed for AlPcS4 content using absorption spectroscopy.

Liposome irradiation

After Sephadex exclusion, air-saturated liposome suspensions were irradiated at 670 nm using a B&W Tek BWF1-670 diode laser while magnetically stirring. The radiant dose was measured by chemical actinometry using AlPcS4 in phosphate buffer (pH 7.4) + 1%Triton X100 for which the quantum yield for the formation of $^1O_2$ is 0.43 at 673 nm [38]. For this purpose, the destruction of furoic acid (Δ[furoic]) was used as $^1O_2$ probe [39,40], using a sufficiently large concentration of furoic acid to trap all singlet oxygen. The latter was obtained from a graph of Δ[furoic] vs. furoic concentration extrapolated to a constant maximum value of Δ[furoic]. Furoic consumption was determined by HPLC as described elsewhere [41].

Nitrite and nitrate detection outside liposomes

Irradiated liposome samples were first centrifuged as described above. Nitrite + nitrate analyses were performed using the Griess assay, as described previously [42,43]. For this purpose, an aliquot of 100 μLs of the supernatant of the irradiated sample was mixed with 100 μLs of Griess reagent, stirred with this reagent for 5 minutes, and the absorbance measured at 540 nm. Nitrite concentration was determined using a nitrite calibration curve. Nitrate was measured using the same method after reduction of nitrate to nitrite by nitrate reductase [43].

$^1O_2$ detection outside liposomes

In order to report singlet oxygen formation outside the liposome, furoic acid (a membrane impermeable probe), was used [44,45]. $^1O_2$ was detected using furoic acid consumption, determined by HPLC as described elsewhere [41].

Aerobic photosensitized cytotoxicity of liposomes against A2780CP20 cells

The derivation, source, and propagation of human epithelial ovarian cancer platinum-resistant A2780CP20 cell line were described previously [46]. Cell line resistance was developed by sequential exposure of the A2780 cell line to increasing concentrations of cisplatin [47]. All experiments were done with 70% to 80% confluent cultures. Cell viabilities were measured after irradiation at 670 nm in the presence of 57.44DOPC:37.44CHOL:5DSPE(2000)PEG:0.13DSPE-PEG(5000)-Folate liposomes containing DETAPAC, AlPcS4, in the absence and presence of GSNO in glycine buffer (pH 8.7). For this purpose, cells were plated in black plastic 96-well plates with a transparent bottom (Fisher Scientific) at a density of ca. 5,000 cells/100 uL medium/well and allowed to form monolayers for 24 hours in RPMI 1640 medium. Then, cells were washed with folate-deficient RPMI-1640 and incubated for 3 hours. To these, liposomes were added and incubated for 2 hours. After this period of time, cells were washed with folate-deficient RPMI-1640 to remove any unbound liposome. Cells were then irradiated in groups of four wells, with empty wells between the treated groups to ensure that each group of wells was receiving the correct dose of light, as reported previously [48]. A diode laser system with variable power (0 to 300 mW, B&W Tek Inc) was used in these studies, with a wavelength of 670 nm. The beam was delivered through a 100 μm optical fiber. This beam expands to a circular area of approximately 2 cm of diameter at a distance of 4 cm from the tip of the optical fiber. The cell plate was localized at that distance from the fiber tip. This setup has been previously used in PDT studies with cells [48–52]. Cells were then washed with normal RPMI1640 and left incubating in the dark for 24 hours. After that period, cells were washed with Alamar Blue-containing RPMI 1640 and left incubating for 3 hours. Cell viability was then evaluated by measuring the absorbance of each well at 540 and 630 nm as reported elsewhere [53,54].

Cells and culture conditions

The human epithelial ovarian cancer cells A2780 was purchased from the European Collection of Cell Cultures (ECACC). A2780CP20 were kindly gifted by Dr. Anil K. Sood (MD Anderson Cancer Center, Houston, TX). A2780CP20 cells are the cisplatin resistant counterparts of A2780. These cells are human cell lines commonly used in the ovarian cancer research field [55,56] and since these are cisplatin resistant it is important to know if these will be sensitive to an alternative therapy such as the one described here. Cells were maintained in RPMI-1640 (HyClone, Logan, UT) supplemented with 10% FBS and 1% antibiotics. For experiments, all cells were kept at 37°C and 5% CO_2 atmosphere. Experiments were performed at 60–80% confluency.

Western blot analysis for folate receptor alpha (FRα) measurements

Western blots analysis was performed as reported earlier [57]. Briefly, A2780 and A2780CP20 cells were collected and washed with phosphate buffer saline (PBS) and stored at −80°C until used. Protein extraction was performed as previously reported [57]. Protein samples were subjected to SDS-PAGE and transferred to polyvinylidene difluoride membranes in 25 mM Tris, 192 mM glycine. Membranes were blocked with 5% nonfat dry milk in PBS and 0.05% Tween 20 and probed with FRα primary antibody (Human FOLR1 Antibody; R&D cat MAB5646, Minneapolis, MN). The secondary antibody was an anti-mouse and anti-rabbit IgG horseradish peroxidase (HRP) (Cell Signaling, Beverly, MA) in a 1:1,000 dilution. Blots were developed with enhanced chemiluminescence (ECL) reagent (GE Healthcare, Piscataway, NJ) and autoradiography using a hemiDoc Gel Imaging System (BioRad).

FRα binding determination

A2780CP20 cells (5 X 10^4 cells/mL) were plated into Lab-Tek Chamber Slides (Thermo-Fisher) and incubated overnight at 37°C, 5% CO_2 in a humid atmosphere (normal cell conditions). The next day cells were washed three times with PBS and then treated with liposome nanoparticles and diluted in PBS buffer with a final lipid concentration of 0.4 mM. Cells were then incubated with liposomes for 15 min. The cells were then washed three times with PBS to remove unbound nanoparticles. Cells were then fixed, nuclei were counterstained with DAPI (1:5000), and slides were mounted with Permafluor Mountant (Thermo Fisher). Cells were observed under a Nikon Eclipse E400 fluorescent microscope, and pictures were taken with the Nikon DS-Qi2 Camera at 20x magnification.

Statistical analyses—Statistical analysis was performed using paired *t*-tests, between different experiment or sample conditions, at an overall significance level of 0.05. Graph and statistical analysis were done using GraphPad Prism (San Diego, CA).

Results and discussion

Dye concentration optimization

In order to optimize the absorption of photons within liposomes, AlPcS4 concentration was increased while NO production was monitored amperometrically, i. e. initial rates of photosensitized NO production from GSNO were determined as a function of dye concentration, Fig. 1. Since NO production rates increased with PS concentration, the largest dye concentration, 900 μM, was used in this work. Since AlPcS4 is a tetraanionic PS, its aggregation is strongly diminished, as reported previously [58], and thus more dye species are available for light absorption and consequent reactivity, as opposed to hydrophobic dyes.

Liposome physical properties

Liposome sizes, polydispersity indexes (PDIs) and zeta potentials are shown on Table 1. Low PDI values were detected, indicating excellent liposome size homogeneities before irradiation. Diameters near 100 nm were obtained, as expected. Encapsulation efficiencies are also shown in Table 1. The latter were about the same in the absence or presence of pegylation. Encapsulation of relatively large concentrations of an anionic species is not

unprecedented. For example, a large concentration of calcein, an anionic compound, is commonly used to detect liposome membrane leakage [59].

Liposome destabilization after photoirradiation

The production of NO gas from GSNO should promote membrane destabilization and thus NO and $^1O_2$ release. In order to test if destabilization of these liposomes occurs after photoirradiation, liposome particle size distributions were measured after incubating these liposomes under dark and after photoirradiation. Liposome disruption evidence is based on the observed differential light scattering (DLS) patterns detected of irradiated and non-irradiated samples containing 6DOPC:4CHOL liposomes, Fig. 2. A very broad distribution of particle diameters with small populations are detected after 10.6 J of irradiation at 670 nm, Fig. 2(b)), as compared to the opposite if the sample is left incubating under dark the same period of time, Fig. 2(a). Thus, both lipid oxidation and NO release may be contributing to such a large dispersion of particle sizes. However, if oxygen is excluded from the sample, a wide distribution of particle sizes is also observed (Fig. 2 (c)) indicating that NO release is disrupting liposomes, an observation not detected in the absence of GSNO under anoxic conditions. An increase in particle size distribution is also observed if GSNO is excluded under aerobic, but not under anaerobic conditions, (Fig. 2(d)) thus indicating that lipid oxidation by ROS also disrupts the liposome structure, as expected. Thus, in addition to liposome oxidation, NO release could also be contributing to liposome particle size heterogeneity. In fact, from the outstanding heterogeneity of particle sizes shown in Fig. 2 (b), it seems that NO release acts synergically with $^1O_2$ in liposome structure degradation. However, pegylated liposomes are not degraded as much as the non-pegylated liposomes, Fig. 2(f), although the distribution of pegylated liposome sizes is broader with a larger DPI value than that of non-pegylated liposomes, indicating that liposome openning and resizing has occurred. Those events should promote liposome release of NO and singlet oxygen from both the pegylated and the non-pegylated liposomes, especially from the non-pegylated liposome. The difference in behavior between non-pegylated and pegylated liposomes could be ascribed to an increase in membrane rigidness due to liposome pegylation [60–62].

$^1O_2$ detection outside liposomes

Both $^1O_2$ and NO could be produced inside the liposomes and a fraction of these species may diffuse outside the liposome. However, if the liposome is disrupted during photoirradiation, the photosensitized production of both NO and $^1O_2$ could also be occurring outside the liposome. In any case, only the species $^1O_2$ and NO located outside the liposome have the potential to exert their toxic effect. In order to detect $^1O_2$ outside the liposomes, an anionic probe, furoic acid, was used to prevent its entrance into the liposomes [39,40]. Mole ratios of $^1O_2$ to PL and of NO to PL are shown in Table 2 for the different liposomes studied here after 10.6 J of laser irradiation. According to these data, a more restricted release of NO and photosensitizer is observed for the pegylated as compared to the non-pegylated liposome. However, this amount of NO might be sufficient to aid in the cytotoxicity of NO and at the tumor tissue. If GSNO is excluded from the 57.5DOPC:37.5CHOL:5.0PEG liposome, the amount of $^1O_2$ detected outside the liposome is about half the value detected if GSNO is included, Table 2. *Thus, it can be observed that singlet oxygen production outside the liposome is largely enhanced if GSNO is present inside the pegylated liposome*

as compared to GSNO absence. The latter is consistent with the observation that GSNO is able to induce liposome particle distribution heterogeneity even in the absence of oxygen, as discussed above. This is a desirable characteristic, since more singlet oxygen will be available for its toxic activity at the tumor site if GSNO is also included. As described above, Figure 2(f) shows that pegylated liposome particles are not degraded as much as with the non-pegylated liposomes. Therefore, the distribution of liposome sizes is broader with a large DPI value, indicating that liposome opening and resizing has occurred, thus enabling an enhanced exit of singlet oxygen.

NO detection outside the liposomes

When 6DOPC:4CHOL liposomes were irradiated during increasing periods of time, at constant light intensity, the amount of nitrite + nitrate (an indirect measure of NO concentration) released outside the liposome increases with irradiation energy dose, Fig. 3. Near 11 % of the nitrite + nitrate concentration corresponds to nitrate, as detected using nitrate reductase. The liposomal leakage %, expressed as AlPcS4 % leakage, also increases with irradiation extent, Fig. 3. In comparison, the amounts of nitrite + nitrate produced and the AlPcS4 release % in samples left under dark, during the same time extent used for irradiation, were negligible.

Photosensitized toxicity against A2780CP20 ovarian cancer cells

A2780CP20 cells express folate receptor alpha (FRα), as determined by Western Blot, Fig. 4A. [63]. A2780 cells were used here to confirm that acquisition of resistance did not alter the expression of FRα. Fig 4B shows that the used antibody is specific for the FRα because not bands were observed with the secondary antibody only. The Fig 4C confirmed also that the antibody is specific for the FRα because when the membrane was preincubated with recombinant FRα protein not bands were observed. These results suggest that our folate liposome preparations can be internalized through this receptor. Thus, we used the cisplatin resistant A2780CP20 cells since photodynamic therapy (PDT) is being tested for the treatment of a variety of solid tumors including metastatic ovarian cancer [64–66]. Using 57.44DOPC:37.44CHOL:5DSPE(2000)PEG:0.13DSPE-PEG(5000)-Folate liposomes, promising results were observed, Fig. 5. Increasing liposome concentrations, at constant light dose, was used in order to increase NO concentrations to be released. These results show that even pegylated liposomes (which are rigid) are also able to photosensitize the killing of these cells, as predicted from the liposome properties described above, as compared to control samples under dark. *An enhancing role of GSNO in this therapy against A2780CP20, cisplatin-resistant cells, is observed*, Fig. 5, i. e., at least half cell viability in the presence of GSNO *vs* its absence is detected under the conditions used. However, this enhancement stays approximately constant after 0.1 mM phospholipid concentration. The latter could be due to folate receptors being saturated even at 0.1 mM lipid concentration. Thus, a further increase in liposome concentration will not decrease further cell viability. However, increasing the irradiation dose further decreased cell viability, Fig. 6.

If cells were irradiated with increasing light fluences at the highest liposome concentration used, cell viability decreases with light fluence increase, Fig. 6. In addition, liposomes

containing GSNO show better photocytotoxic activity than liposomes without GSNO, where this difference in activity increases with radiation fluence extent.

Internalization of liposomes into A2780CP20 cells

Fig. 7 shows in vitro cellular uptake of liposomes containing folate, Fig. 7(a), and without folate, Fig. 7(b). The left panel of Fig. 7 shows cell nuclei stained by DAPI (nuclear fluorescent dye) while the middle panel shows the localization of the liposome dye within cells. Folate-containing liposomes were able to effectively internalize (colocalized) in cells as shown in middle and right panel of Fig. 7, respectively. On the other hand, liposomes without folate did not internalize the cells, which indicates that folate is needed for effective delivery of the liposomes inside cells.

In summary, folate-conjugated liposomes containing the PS dye AlPcS4 and GSNO photosensitize the normoxic killing of A2780CP20 ovarian cancer cells. This activity decreases if GSNO is not present in those liposomes. Evidence provided indicates that this type of liposome emits NO and singlet oxygen when irradiated at 670 nm. However, phthalocyanine dyes are known to also produce superoxide ions, $O_2^{\cdot -}$, and thus H_2O_2 and OH radicals, via a Type I photochemical pathway [67].

Furthermore, superoxide reaction with NO will generate peroxynitrite [68]. Thus, some of those ROS and RNS species, if not all, could have a role in the enhanced cell killing activity shown in this work. Since NO can enhance PDT efficacy in hypoxic tumors owing to the ability of NO in freely diffusing into deep hypoxic tumor site [14], the use of folate-conjugated liposomes containing AlPcS4 + GSNO might be a convenient carrier in the PDT of A2780CP20 or other solid tumors. Thus, the potential advantage of the formulation presented here, as compared to previous works, is the synergistic behavior in singlet oxygen and NO production and toxicities of the tumor-targeted nanoparticles. Scheme 1 summarizes the results described in this work.

Acknowledgments:

We would like to thank Robert Rabelo for the construction of some graphs using prism.

Funding:

This work was supported in part by the National Institute on Minority Health and Health Disparities (NIMHD) CCRHD (U54MD007600); institutional seed funds from the UPR Comprehensive Cancer Center.

REFERENCES

[1]. Shen Z, Ma Q, Zhou X, Zhang G, Hao G, Sun Y et al. (2021) Strategies to improve photodynamic therapy efficacy by relieving the tumor hypoxia environment. NPG Asia Mater, 13:1–19.

[2]. Di Nicola M, Williams BK Jr, Hua J, Bekerman VP, Mashayekhi A, Shields JA et al. (2021) Photodynamic Therapy (PDT) for Retinal Hemangioblastoma: Treatment Outcomes in 17 Consecutive Patients. Ophthalmol Retina,.

[3]. Rak J, Pouckova P, Benes J, Vetvicka D (2019) Drug delivery systems for phthalocyanines for photodynamic therapy. Anticancer Res 39:3323–39. [PubMed: 31262853]

[4]. Shi Z, Meng X, Zhang K, Tang S, Zhang C, Yang Z et al. (2021) Engineering Structural Metal–Organic Framework for Hypoxia-Tolerant Type I Photodynamic Therapy against Hypoxic Cancer. ACS Mater Lett 3:781–9.

[5]. Nwogu C, Kloc A, Attwood K, Bshara W, Durrani F, Pandey R (2021) Porfimer Sodium Versus PS785 for Photodynamic Therapy (PDT) of Lung Cancer Xenografts in Mice (A Novel Agent for Lung Cancer PDT). J Surg Res 263:245–50. [PubMed: 33713956]

[6]. Derycke ASL, de Witte PAM (2004) Liposomes for photodynamic therapy. Adv Drug Deliv Rev 56:17–30. [PubMed: 14706443]

[7]. Torchilin VP (2012) Multifunctional nanocarriers. Adv Drug Delivery Rev, 64:302–15.

[8]. Bovis MJ, Woodhams JH, Loizidou M, Scheglmann D, Bown SG, MacRobert AJ (2012) Improved in vivo delivery of m-THPC via pegylated liposomes for use in photodynamic therapy. J Control Release 157:196–205. [PubMed: 21982898]

[9]. Huang Z, Fu J, Zhang Y (2017) Nitric oxide donor-based cancer therapy: advances and prospects. J Med Chem 60:7617–35. [PubMed: 28505442]

[10]. Ma J, Wu H, Li Y, Liu Z, Liu G, Guo Y et al. (2018) Novel core-interlayer-shell DOX/ZnPc Co-loaded MSNs@ pH-Sensitive CaP@ PEGylated liposome for enhanced synergetic chemo-photodynamic therapy. Pharm Res 35:1–12.

[11]. Bonavida B, Baritaki S, Huerta-Yepez S, Vega MI, Chatterjee D, Yeung K (2008) Novel therapeutic applications of nitric oxide donors in cancer: roles in chemo-and immunosensitization to apoptosis and inhibition of metastases. Nitric Oxide 19:152–7. [PubMed: 18477483]

[12]. Muntané J, Angel J, Marín LM, Padillo FJ (2013) Nitric oxide and cell death in liver cancer cells. Mitochondrion 13:257–62. [PubMed: 23009756]

[13]. Mocellin S, Bronte V, Nitti D (2007) Nitric oxide, a double edged sword in cancer biology: searching for therapeutic opportunities. Med Res Rev 27:317–52. [PubMed: 16991100]

[14]. Wan S-S, Zeng J-Y, Cheng H, Zhang X-Z (2018) ROS-induced NO generation for gas therapy and sensitizing photodynamic therapy of tumor. Biomaterials 185:51–62. [PubMed: 30218836]

[15]. Negri LB, Martins TJ, da Silva RS, Hamblin MR (2019) Photobiomodulation combined with photodynamic therapy using ruthenium phthalocyanine complexes in A375 melanoma cells: Effects of nitric oxide generation and ATP production. J Photochem Photobiol B: Biol 198:111564.

[16]. Rapozzi V, Della Pietra E, Zorzet S, Zacchigna M, Bonavida B, Xodo LE (2013) Nitric oxide-mediated activity in anti-cancer photodynamic therapy. Nitric Oxide 30:26–35. [PubMed: 23357401]

[17]. Xiang H-J, Deng Q, An L, Guo M, Yang S-P, Liu J-G (2016) Tumor cell specific and lysosome-targeted delivery of nitric oxide for enhanced photodynamic therapy triggered by 808 nm near-infrared light. Chem Commun 52:148–51.

[18]. Monroy M, Tipgunlakant P, Simonis U, Esquerra R (2014) Nitric oxide and its role in photodynamic therapy. Cancer Res, AACR. 74(19 Suppl):Abstract nr 5111.

[19]. Heinrich TA, Tedesco AC, Fukuto JM, da Silva RS (2014) Production of reactive oxygen and nitrogen species by light irradiation of a nitrosyl phthalocyanine ruthenium complex as a strategy for cancer treatment. Dalton Trans 43:4021–5. [PubMed: 24452093]

[20]. Singh RJ, Hogg N, Joseph J, Kalyanaraman B (1995) Photosensitized decomposition of S-nitrosothiols and 2-methyl-2-nitrosopropane. Possible use for site-directed nitric oxide production. FEBS Lett 360:47–51. [PubMed: 7875299]

[21]. Juzenas P, Juzeniene A, Rotomskis R, Moan J (2004) Spectroscopic evidence of monomeric aluminium phthalocyanine tetrasulphonate in aqueous solutions. J Photochem Photobiol, B 75:107–10. [PubMed: 15246357]

[22]. Filonenko EV, Sokolov VV, Chissov VI, Lukyanets EA, Vorozhtsov GN (2008) Photodynamic therapy of early esophageal cancer. Photodiagnosis Photodyn Ther 5:187–90. [PubMed: 19356654]

[23]. Trushina OI, Novikova EG, Sokolov VV, Filonenko EV, Chissov VI, Vorozhtsov GN (2008) Photodynamic therapy of virus-associated precancer and early stages cancer of cervix uteri. Photodiagnosis Photodyn Ther 5:256–9. [PubMed: 19356666]

[24]. Tran DL, Le Thi P, Park KD In situ Generation of Nitric Oxide from Heparinized Surfaces for Enhanced Cardiovascular Therapy.

[25]. Baydoun M, Moralès O, Frochot C, Ludovic C, Leroux B, Thecua E et al. (2020) Photodynamic Therapy Using a New Folate Receptor-Targeted Photosensitizer on Peritoneal Ovarian Cancer

Cells Induces the Release of Extracellular Vesicles with Immunoactivating Properties. J Clin Med 9:1185. [PubMed: 32326210]

[26]. Luan S, Tran NT, Xue HY, Wong HL (2021) Development of a high payload, cancer-targeting liposomes of methyl aminolevulinate for intraoperative photodynamic diagnosis/therapy of peritoneal carcinomatosis. Int J Pharm 602:120612. [PubMed: 33905866]

[27]. Timmermans M, Sonke GS, Van de Vijver KK, Van der Aa MA, Kruitwagen R (2018) No improvement in long-term survival for epithelial ovarian cancer patients: a population-based study between 1989 and 2014 in the Netherlands. Eu J Cancer 88:31–7.

[28]. Hart TW (1985) Some observations concerning the s-nitroso and s-phenylsulphonyl derivatives of l-cysteine and glutathione. Tetrahedron Let 26:2013–6.

[29]. McCord JM, Fridovich I (1969) Superoxide dismutase. An enzymic function for erythrocuprein (hemocuprein). J Biol Chem 244:6049–55. [PubMed: 5389100]

[30]. Logan LPH, Gummet PA, Misiewicz JJ, Karim QN, Walker MM, Baron GH (1991) One week erradication regime for Helicobacter pylori. Lancet 11:1449–52.

[31]. Qualls MM, Thompson DH (2001) Chloroaluminum phthalocyanine tetrasulfonate delivered via acid-labile diplasmenylcholine-folate liposomes: Intracellular localization and synergistic phototoxicity. Int J Cancer 93:384–92. [PubMed: 11433404]

[32]. Maniatis T, Fritsch EF, Sambrook J (1982) Molecular Cloning. A Laboratory Manual. Cold Spring Harbor Laboratory Press, New York. p. 466–7.

[33]. Sibata CH, Colussi VC, Oleinick NL, Kinsella TJ (2001) Photodynamic therapy in oncology. Expert Opin Pharmacother 2:917–27. [PubMed: 11585008]

[34]. Aygun A, Torrey K, Kumar A, Stephenson LD (2012) Investigation of factors affecting controlled release from photosensitive DMPC and DSPC liposomes. Appl Biochem Biotech 167:743–57.

[35]. Singh RJ, Hogg N, Joseph J, Kalyanaraman B (1996) Mechanism of nitric oxide release from S-nitrosothiols. J Biol Chem 271:18596–603. [PubMed: 8702510]

[36]. New RRC (1990) Liposomes: A Practical Approach. In: Rickwood Hames BDD, editor. The Practical Approach Series, Oxford University Press, New York. p. 44–8.

[37]. Xie Y, Ye L, Zhang X, Cui W, Lou J, Nagai T et al. (2005) Transport of nerve growth factor encapsulated into liposomes across the blood–brain barrier: In vitro and in vivo studies. J Control Release 105:106–19. [PubMed: 15893839]

[38]. Fernandez JM, Bilgin MD, Grossweiner LI (1997) Singlet oxygen generation by photodynamic agents. J Photochem Photobiol B 37:131–40.

[39]. Fabregat V, Burguete MI, Galindo F, Luis SV (2014) Singlet oxygen generation by photoactive polymeric microparticles with enhanced aqueous compatibility. Environ Sci Pollut R 21:11884–92.

[40]. Urakami H, Zhang K, Vilela F (2013) Modification of conjugated microporous poly-benzothiadiazole for photosensitized singlet oxygen generation in water. Chem Commun 49:2353–5.

[41]. Coelho C, Guyot G, Ter Halle A, Cavani L, Ciavatta C, Richard C (2011) Photoreactivity of humic substances: relationship between fluorescence and singlet oxygen production. Environ Chem Lett 9:447–51.

[42]. Green LC, Wagner DA, Glogowski J, Skipper PL, Wishnok JS, Tannenbaum SR (1982) Analysis of nitrate, nitrite, and [15N]nitrate in biological fluids. Anal Biochem 126:131–8. [PubMed: 7181105]

[43]. Misko TP, Schilling RJ, Salvemini D, Moore WM, Currie MG (1993) A fluorometric assay for the measurement of nitrite in biological samples. Anal Biochem 214:11–6. [PubMed: 7504409]

[44]. Ji Y, Akerboom TP, Sies H, Thomas JA (1999) S-nitrosylation and S-glutathiolation of protein sulfhydryls by S-nitroso glutathione. Arch Biochem Biophys 362:67–78. [PubMed: 9917330]

[45]. Smyth DG, Nagamatsu A, Fruton JS (1960) Some Reactions of N-Ethylmaleimide1. J Am Chem Soc 82:4600–4.

[46]. Sood AK, Seftor EA, Fletcher MS, Gardner LMG, Heidger PM, Buller RE et al. (2001) Molecular determinants of ovarian cancer plasticity. Am J Pathol 158:1279–88. [PubMed: 11290546]

[47]. O'Dwyer PJ, Hamilton TC, Young RC, LaCreta FP, Carp N, Tew KD et al. (1992) Depletion of glutathione in normal and malignant human cells in vivo by buthionine sulfoximine: clinical and biochemical results. J Natl Cancer Inst 84:264–7. [PubMed: 1734088]

[48]. Pogue BW, O'Hara JA, Demidenko E, Wilmot CM, Goodwin IA, Chen B et al. (2003) Photodynamic therapy with verteporfin in the radiation-induced fibrosarcoma-1 tumor causes enhanced radiation sensitivity. Cancer Res 63:1025–33. [PubMed: 12615718]

[49]. Hu Z, Rao B, Chen S, Duanmu J (2010) Targeting tissue factor on tumour cells and angiogenic vascular endothelial cells by factor VII-targeted verteporfin photodynamic therapy for breast cancer in vitro and in vivo in mice. BMC Cancer 10:235. [PubMed: 20504328]

[50]. Colussi VC, Feyes DK, Mulvihill JW, Li Y-S, Kenney ME, Elmets CA et al. (1999) Phthalocyanine 4 (Pc 4) Photodynamic Therapy of Human OVCAR-3 Tumor Xenografts. Photochem Photobiol 69:236–41. [PubMed: 10048316]

[51]. Chiu SM, Xue LY, Lam M, Rodriguez ME, Zhang P, Kenney ME et al. (2010) A requirement for bid for induction of apoptosis by photodynamic therapy with a lysosome-but not a mitochondrion-targeted photosensitizer. Photochem Photobiol 86:1161–73. [PubMed: 20553412]

[52]. Paul B, Rajaputra P and You Y (2011) In vitro and in vivo photodynamic activity of core-modified porphyrin IY69 using 690 nm diode laser. Photochem Photobiol 87:1468–73. [PubMed: 21854396]

[53]. Al-Nasiry S, Geusens N, Hanssens M, Luyten C, Pijnenborg R (2007) The use of Alamar Blue assay for quantitative analysis of viability, migration and invasion of choriocarcinoma cells. Hum Reprod, 22:1304–9. [PubMed: 17307808]

[54]. Echevarría-Vargas IM, Valiyeva F, Vivas-Mejía PE (2014) Upregulation of miR-21 in cisplatin resistant ovarian cancer via JNK-1/c-Jun pathway. PLoS One 9:e97094. [PubMed: 24865582]

[55]. Reyes-González JM, Quiñones-Díaz BI, Santana Y, Báez-Vega PM, Soto D, Valiyeva F et al. (2020) Downstream Effectors of ILK in Cisplatin-Resistant Ovarian Cancer. Cancers 12:880. [PubMed: 32260415]

[56]. Quiñones-Díaz BI, Reyes-González JM, Sánchez-Guzmán V, Conde-Del Moral I, Valiyeva F, Santiago-Sánchez GS et al. (2020) MicroRNA-18a-5p suppresses tumor growth via targeting matrix metalloproteinase-3 in cisplatin-resistant ovarian cancer. Front Oncol 10:2887.

[57]. Báez-Vega PM, Vargas IM, Valiyeva F, Rosado JE, Roman A, Flores J et al. (2016) Targeting miR-21–3p inhibits proliferation and invasion of ovarian cancer cells. Oncotarget 7:36321. [PubMed: 27166999]

[58]. Juzenas P, Juzeniene A, Rotomskis R, Moan J (2004) Spectroscopic evidence of monomeric aluminium phthalocyanine tetrasulphonate in aqueous solutions. J Photochem Photobiol B 75:107–10. [PubMed: 15246357]

[59]. Firsov AM, Kotova EA, Antonenko YN (2018) Calcein leakage as a robust assay for cytochrome c/H 2 O 2–mediated liposome permeabilization. Anal Biochem 52:19–23.

[60]. Hashizaki K, Taguchi H, Itoh C, Sakai H, Abe M, Saito Y et al. (2003) Effects of poly (ethylene glycol)(PEG) chain length of PEG-lipid on the permeability of liposomal bilayer membranes. Chem Pharm Bull (Tokyo) 51:815–20. [PubMed: 12843588]

[61]. Gabizon AA, Shmeeda H, Zalipsky S (2006) Pros and cons of the liposome platform in cancer drug targeting. J Liposome Res 16:175–83. [PubMed: 16952872]

[62]. Dadashzadeh S, Vali AM, Rezaie M (2008) The effect of PEG coating on in vitro cytotoxicity and in vivo disposition of topotecan loaded liposomes in rats. Int J Pharm 353:251–9. [PubMed: 18191511]

[63]. Wen Y, Graybill WS, Previs RA, Hu W, Ivan C, Mangala LS et al. (2015) Immunotherapy targeting folate receptor induces cell death associated with autophagy in ovarian cancer. Clin Cancer Res 21:448–59. [PubMed: 25416196]

[64]. Rizvi I, Anbil S, Alagic N, Celli JP, Zheng LZ, Palanisami A et al. (2013) PDT dose parameters impact tumoricidal durability and cell death pathways in a 3D ovarian cancer model. Photochem Photobiol 89:942–52. [PubMed: 23442192]

[65]. Azaïs H, Estevez JP, Foucher PP, Kerbage Y, Mordon S, Collinet P et al. (2017) Dealing with microscopic peritoneal metastases of epithelial ovarian cancer. A surgical challenge. Surg Oncol 26:46–52. [PubMed: 28317584]

[66]. Azaïs H, Schmitt C, Tardivel M, Kerdraon O, Stallivieri A, Frochot C et al. (2016) Assessment of the specificity of a new folate-targeted photosensitizer for peritoneal metastasis of epithelial ovarian cancer to enable intraperitoneal photodynamic therapy. A preclinical study. Photodiagnosis Photodyn Ther 13:130–8. [PubMed: 26200606]

[67]. Dias LM, Sharifi F, de Keijzer MJ, Mesquita B, Desclos E, Kochan JA et al. (2021) Attritional evaluation of lipophilic and hydrophilic metallated phthalocyanines for oncological photodynamic therapy. J Photochem Photobiol B: Biol 216:112146.

[68]. Kang SH, Chung BY, Park JE, Jeon J, Park YD (2020) Activatable red emitting fluorescent probe for rapid and sensitive detection of intracellular peroxynitrite. Talanta 217:121053. [PubMed: 32498841]

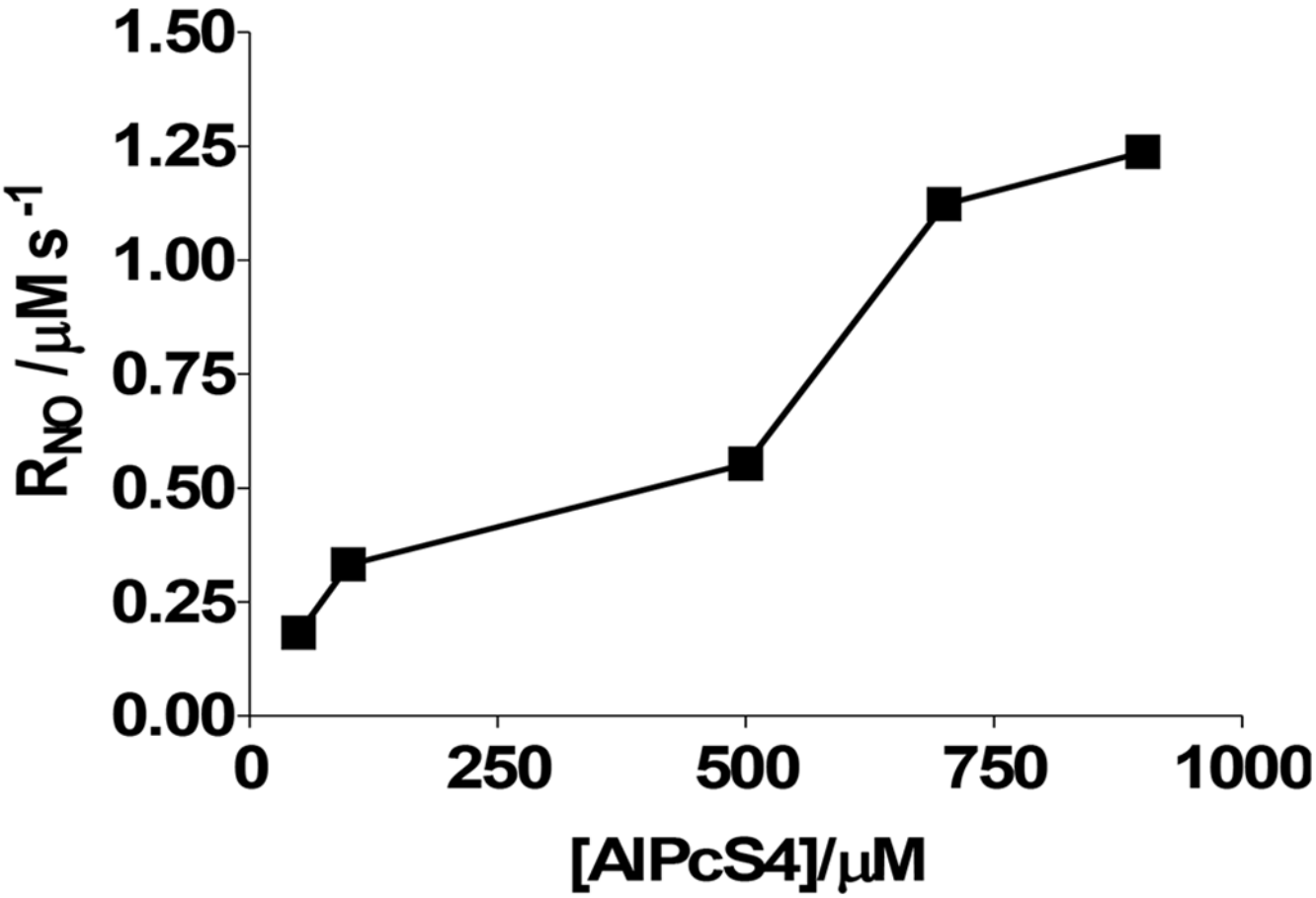

Figure 1.

Initial rates of photosensitized NO production upon irradiation of 60 mM GSNO and AlPcS4 at 670 nm in glycine buffer (pH 8.7) in the presence of 300 uM DTPA and 300 uM neocuproine. Samples were N_2-saturated before starting irradiation. The radiation energy flux used was 70 mJ cm^{-2} s^{-1}.

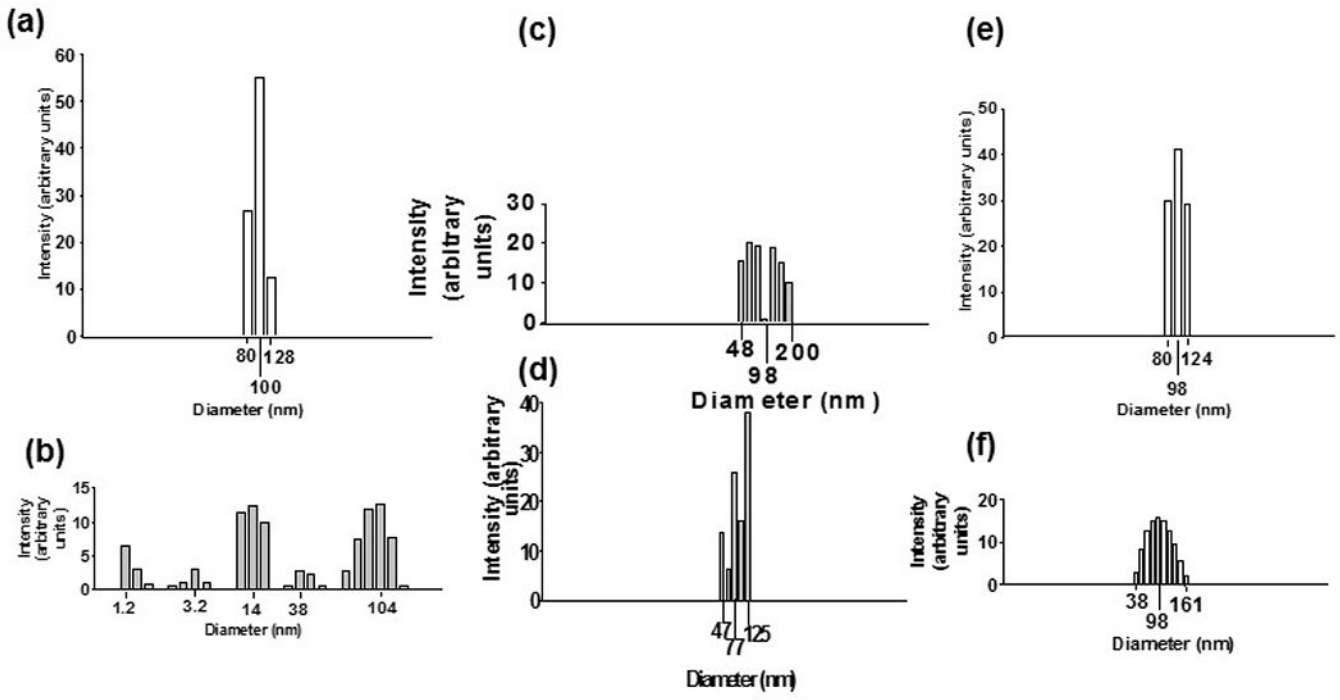

Figure 2.

Particle size distribution of liposomes after 0 (white bars: (a) and (e)) or 10.6 J (colored bars) of irradiation at 670 nm. The liposome used in (a) – (d) is 6DOPC:4CHOL. The liposome used in (e) and (f) is 57.5DOPC:38.5CHOL:5.0PEG. All liposomes with the exception of that in (c) are air-saturated. Bulk concentrations of reagents before extrusion are 900 μM AlPcS4, 60 mM GSNO, 300 μM DETAPAC and 300 μM neocuproine in 20 mM glycine buffer at pH 8.7. (c) N_2-saturated; (d) no GSNO was included. Phospholipid concentration was the same in all samples.

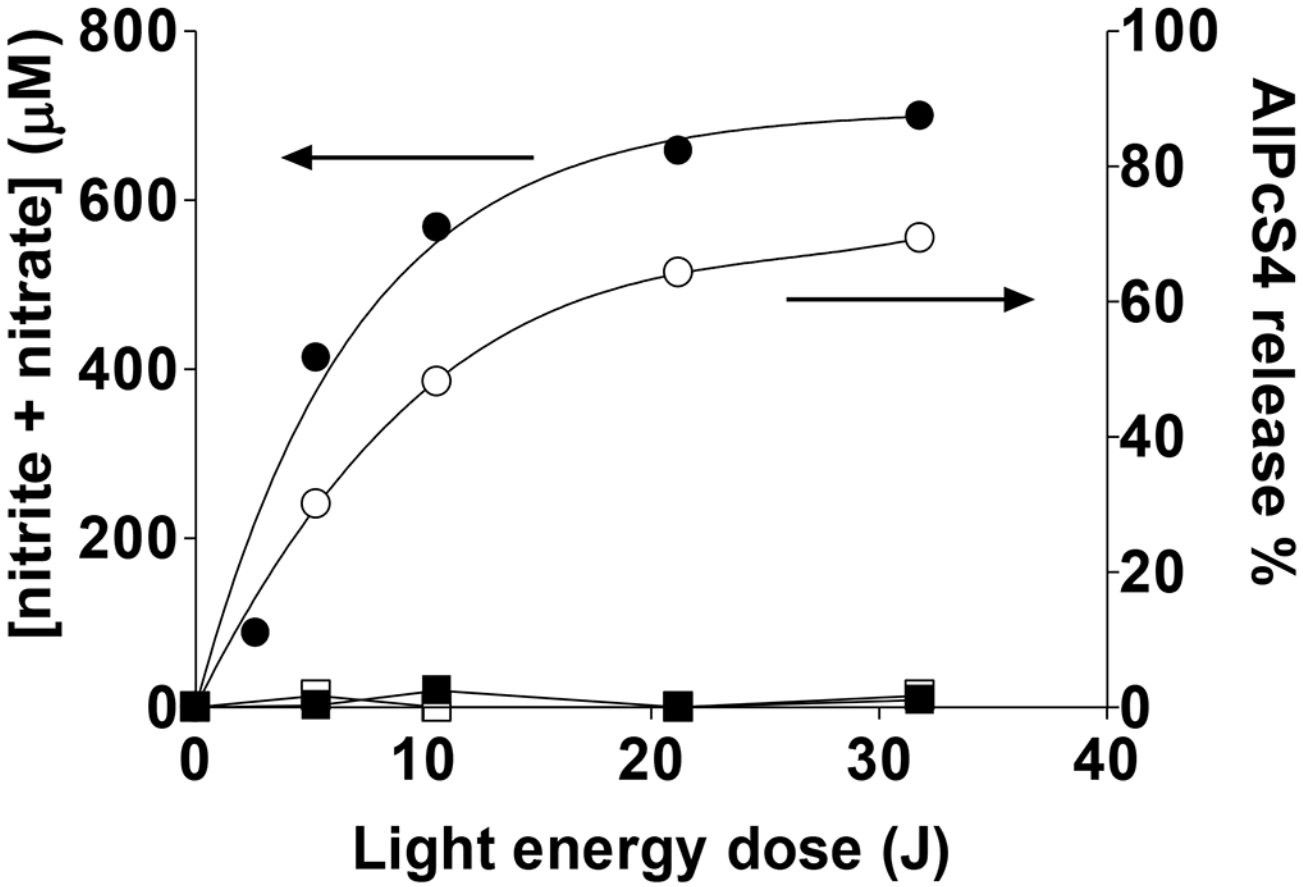

Figure 3.

Nitrite + nitrate production (black symbols) and % AlPcS4 release (white symbols) from 6DOPC:4CHOL liposomes. Samples were irradiated (circles) or not irradiated (squares) at 670 nm. Non-irradiated samples were kept under dark during the time period used for irradiated samples. Bulk concentrations of reagents before liposome extrusion are 900 μM AlPcS4, 60 mM GSNO, 300 μM DETAPAC and 300 μM neocuproine in 20 mM glycine buffer at pH 8.7. Near 11 % of the nitrite + nitrate concentration corresponds to nitrate. NO to phospholipid (PL) mole ratios are shown in Table 2.

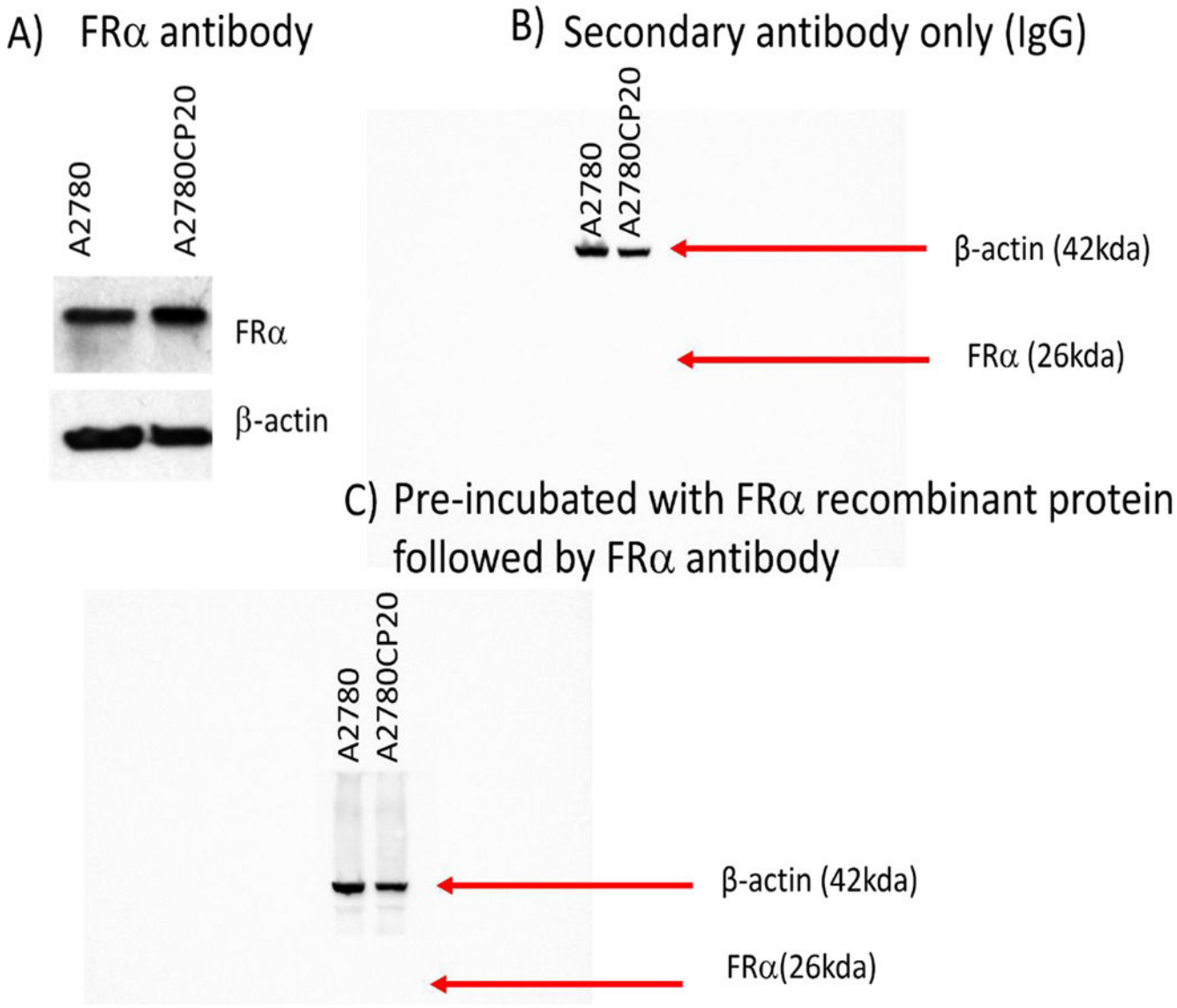

Figure 4.

Western blot analysis of the FRα protein in A2780 and A2780CP20 cells. (**A**) Representative image of a Western blot analysis to detect the FRα levels. Western blots were performed with 50 μg of protein extracts. (**B**) Membranes were incubated with the secondary antibody, only. (**C**) Membrane was first incubated with a recombinant FRα protein an then incubated with the primary antibody followed by incubation with the secondary antibody.

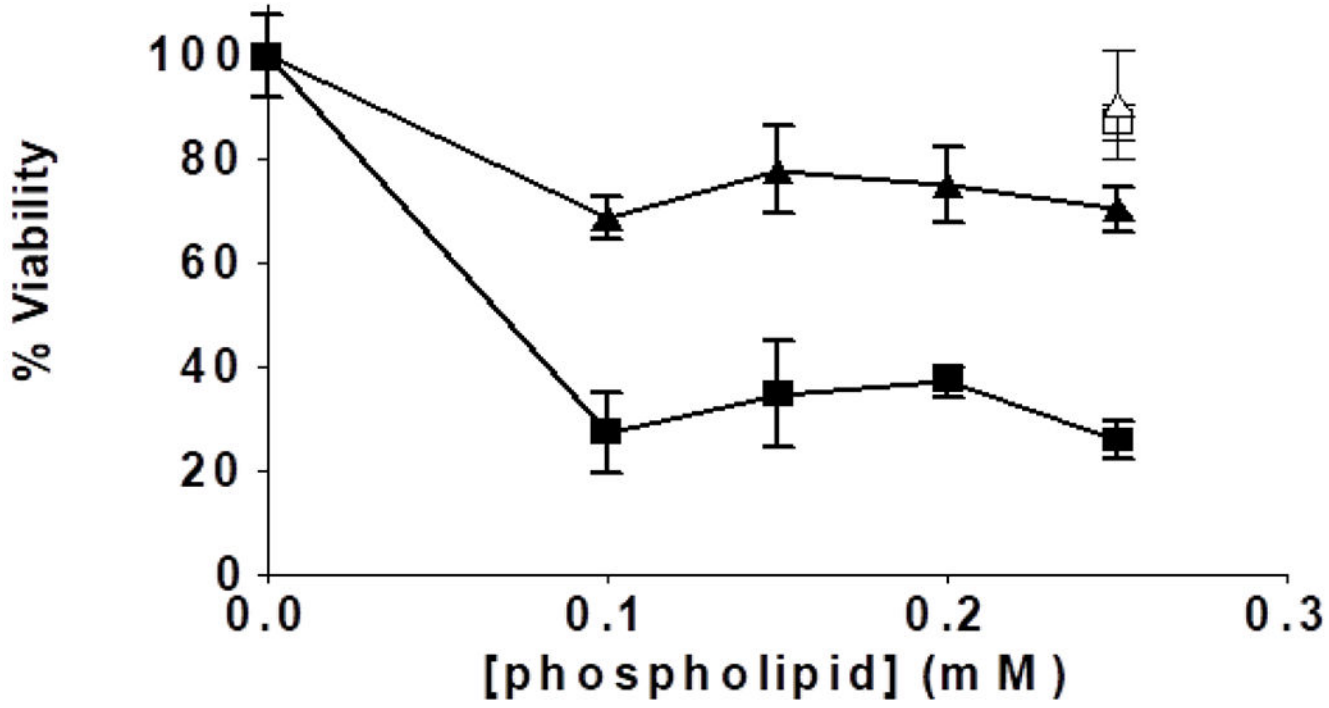

Figure 5.

Role of GSNO in the photosensitized cytotoxicity to A2780CP20 ovarian cancer cells after 1.4 J/cm^2 of irradiation at 670 nm in the presence of different concentrations of 57.44DOPC:37.44CHOL:5DSPE(2000)PEG:0.13DSPE-PEG(5000)-Folate liposomes. Closed (or black) square and triangle symbols correspond to liposomes containing and not containing GSNO, respectively. Open (or white) symbols correspond to samples containing liposomes with 0.25 mM phospholipid with the same composition as those of the corresponding closed symbols and which were kept under dark during all the procedure. Bulk concentrations of reagents before liposome extrusion are 900 μM AlPcS4, 60 mM GSNO, 300 μM DETAPAC and 300 μM neocuproine in 20 mM glycine buffer at pH 8.7. Data presented are averages of 3 determinations ± SEM ($P < 0.05$ in two-tailed paired t-test comparing cell death with and without GSNO).

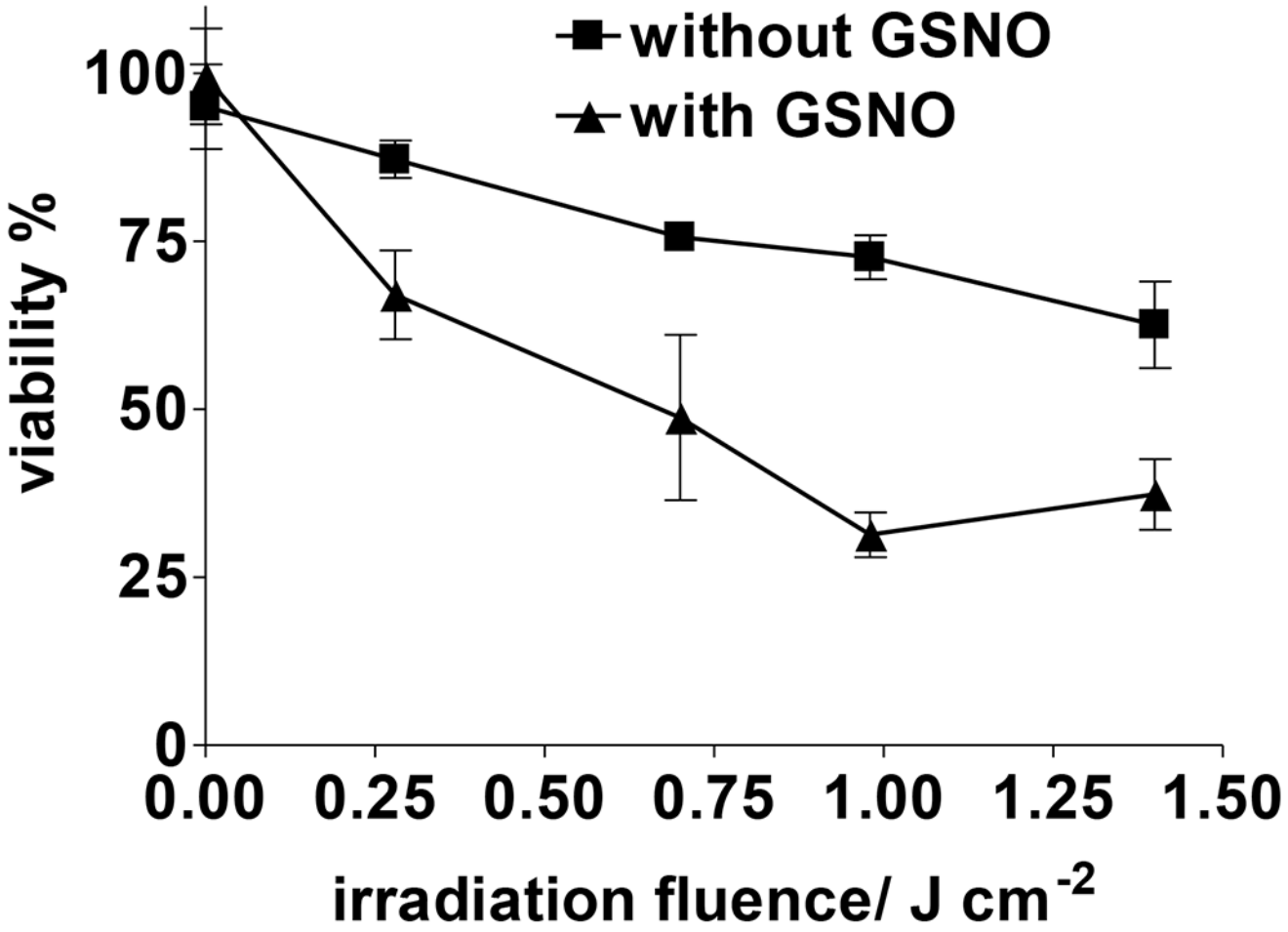

Figure 6.

Role of light fluence and of GSNO presence in the photosensitized cytotoxicity to A2780CP20 ovarian cancer cells upon irradiation at 670 nm in the presence 57.44DOPC:37.44CHOL:5DSPE(2000)PEG:0.13DSPE-PEG(5000)-Folate liposomes at a constant PL concentration of 0.25 mM. Bulk concentrations of reagents before liposome extrusion are 900 μM AlPcS4, 60 mM GSNO, 300 μM DETAPAC and 300 μM neocuproine in 20 mM glycine buffer at pH 8.7. Data presented are averages of 3 determinations ± SEM ($P < 0.05$ in two-tailed paired t-test comparing cell death with and without GSNO).

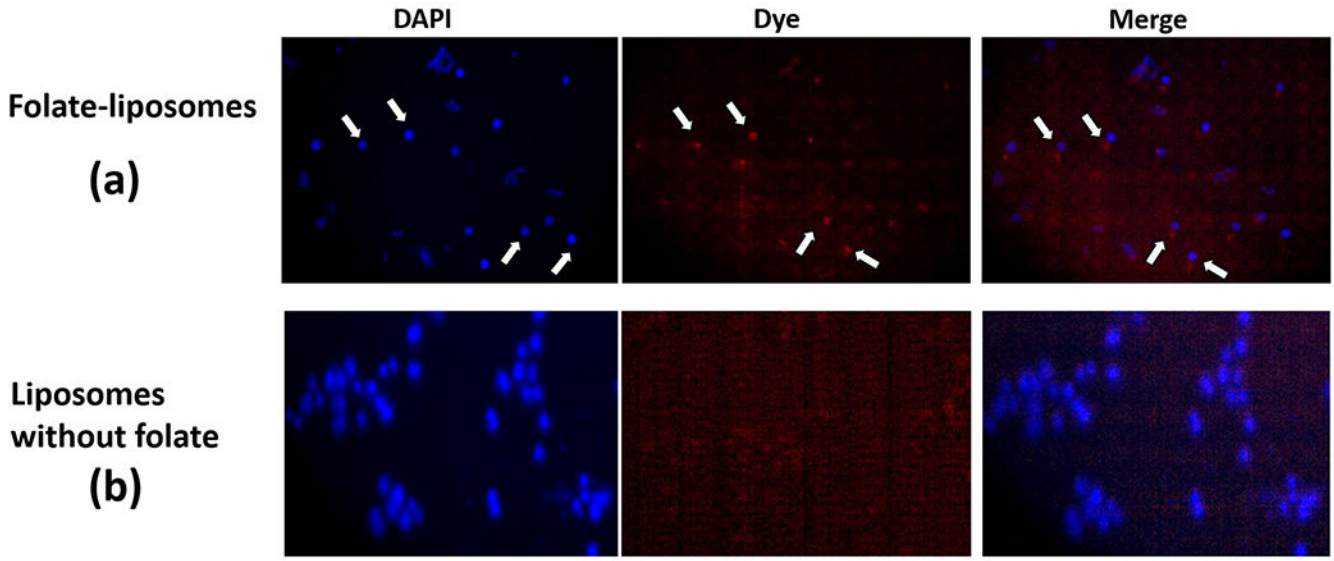

Figure 7.

Representative fluorescence emission intensity images after incubation of A2780CP20 cells with (a) 57.44DOPC:37.44CHOL:5.0PEG:0.13DSPE-PEG(5000)-Folate and (b) 57.5DOPC:37.5CHOL:5.0PEG liposomes, both containing AlPcS4 and GSNO. Procedures are described in MATERIALS AND METHODS.

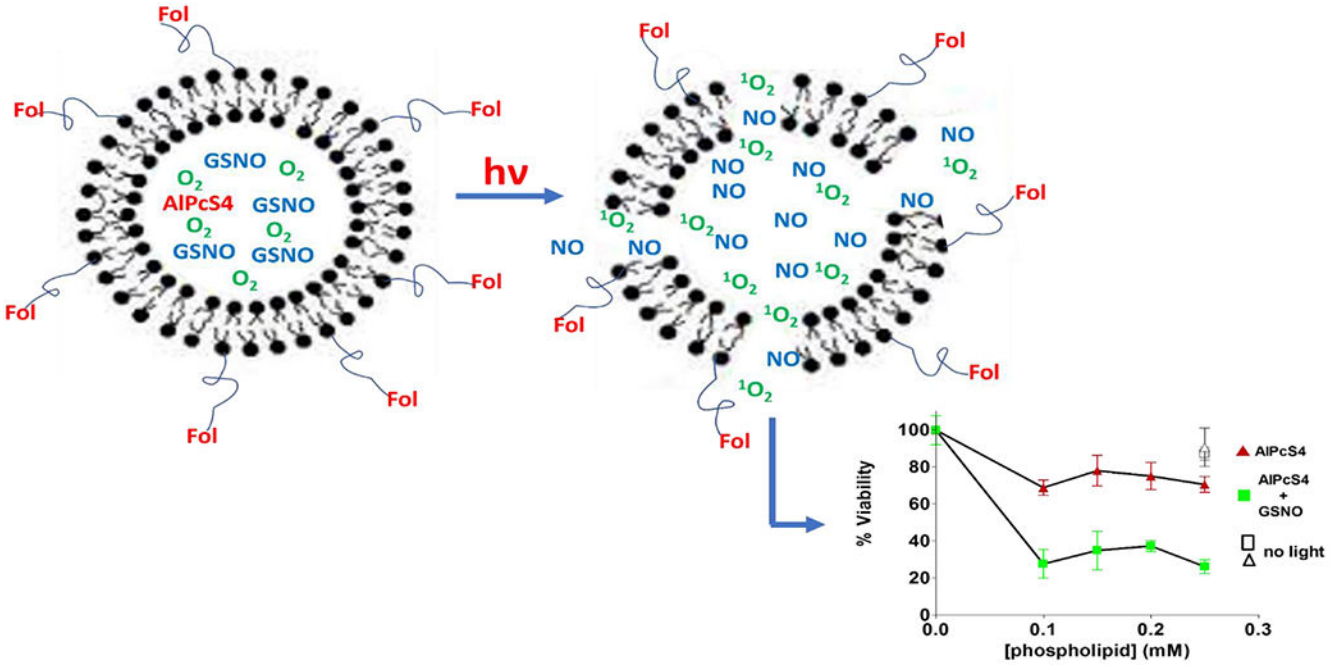

Scheme 1.

Graphical representation of the results described in this work regarding liposome light activation of the liposomes used and the consequent A2780CP20 ovarian cancer cells viabilities.

Table 1.

Liposomes physical properties.[a]

Liposome	Average diameter (nm)	Zeta potential (mV)	PDI[b]	Encapsulation efficiency (%)		Loading capacity[c]	
				AlPcS4	GSNO	AlPcS4	GSNO
6DOPC:4CHOL	98 ± 12	−66 ± 4	0.06 ± 0.02	40 ± 2	37 ± 3	0.036 ± 0.002	2.1 ± 0.3
57.5DOPC:37.5CHOL:5.0PEG	100 ± 18	−72 ± 3	0.06 ± 0.03	39 ± 3	41 ± 4	0.04 ± 0.03	3.3 ± 0.1

Values are means ± SEM of values from at least three replicate determinations.

a. bulk concentrations of reagents before extrusion are 10 mM phospholipid, 900 μM AlPcS4, 60 mM GSNO, 300 μM DETAPAC and 300 μM neocuproine in 20 mM glycine buffer at pH 8.7.;

b. polydispersity index;

c. mol drug/ mol phospholipid after Sephadex extraction.

Table 2.

Mole ratios of released NO and $^1O_2$ to phospholipid (PL) after 10.6 J of irradiation at 670 nm. Liposome properties are shown in Table 1.

Liposome	$^1O_2$ to PL mole ratio[a]	NO to PL mole ratio[a]
60DOPC:40CHOL	*b*	0.063 ± 0.003 (0.001 ± 0.002)[c]
57.5DOPC:37.5CHOL:5.0PEG	0.032 ± 0.004 (0.000 ± 0.000)	0.014 ± 0.004 (0.000 ± 0.000)
57.5DOPC:37.5CHOL:5.0PEG without GSNO	0.013 ± 0.002	-----

a. Values are means ± SEM of values from at least three replicate determinations. NO was determined using Griess assay as nitrite + nitrate. Singlet oxygen was determined using furoic acid as probe.

b. Not determined.

c. Values in parentheses correspond to dark incubation during the same irradiation time period.